SIMULATION OF SELF-INDUCED UNSTEADY MOTION IN THE NEAR WAKE OF A JOUKOWSKI AIRFOIL†

K.N. Ghia*, G.A. Osswald* and U. Ghia**
*Department of Aerospace Engineering and Engineering Mechanics
**Department of Mechanical Engineering
University of Cincinnati
Cincinnati, Ohio 45221/USA

INTRODUCTION

Recent impetus for research in unsteady separated flows stems from a wide range of applications from low- to high- Reynolds number, Re. The physics of high-Re flows, in general, is quite complex and often involves multiple nonuniqueness and chaos, beyond simple unsteady separation. For the low-Re case, e.g. in the manuevering of fighter aircraft at high angle-of-attack in near- and post-stall regime, the vortex interaction dominates the flow field. The passage of vortices over the suction surface and their subsequent shedding leads to self-excited persistently unsteady flows. This flow field is extremely complicated due to the global effect of unsteady separated flow, coupled with the presence of hydrodynamic instabilities which may trigger transition and eventually lead to chaos. Besides supermaneuverability, interest also lies in this low-Re case because of the need for design of efficient airfoil sections for Re in the range of 10^5-10^6, for improving the performance of mini-RPV's (remotely piloted vehicles) operating at low altitudes, jet engine compressor and turbine blades, helicopter rotor blades, etc.

For low-speed viscous flow without body forces, Re is the key similarity parameter. For flow over lifting bodies, the flow pattern is unique and steady for $Re < Re_{cr}$, where Re_{cr} is the value of Re at which transition first occurs. Near and beyond Re_{cr}, the flow is highly unsteady and it becomes imperative that this unsteady flow be better understood. Recent developments in the dynamical theory of low-dimensional nonlinear systems have provided a new and stimulating viewpoint concerning the onset of turbulence, as computer simulations of three or more coupled nonlinear first-order ordinary differential equations have led to chaotic solutions. Such an observation led Ruelle and Takens (1971) to hypothesize that transition to turbulence can be quantitatively explained by deterministic equations. Their work has produced exciting and profound results and the resulting theory has become widely known as the Ruelle-Takens theory of turbulence. They showed mathematically that, for a nonlinear initial-boundary value problem, with a large critical parameter such as Re, chaos resulted from repeated bifurcations of the solution.

† This research was supported, in part, by NASA Grant No. NAG-1-465 and, in part, by AFOSR Grant No. 85-0231.

The chaotic solutions were referred to as "Strange Attractors", to distinguish them from other ordinary attractors such as fixed points and limit cycles, i.e. steady-state and periodic solutions, respectively. The strange attractors are geometric entities in the phase or state space of the governing differential equations. In this context, fixed points are zero-dimensional entities, limit cycles are one-dimensional entities in the sense that they can be parameterized by a single degree of freedom, and strange attractors are more-than-one dimensional, perhaps even of fractional dimension. The important point is that the dimension of a strange attractor is often quite low. Indeed, in this new approach, it is possible that the underlying mechanism responsible for chaotic behavior can be characterized by only a few degrees of freedom. This new theory contradicts the earlier statistical theory which treats turbulence as a broad (i.e., many degrees of freedom) spectrum of periodic disturbances. But it is conjectured that it should include the secondary instability theory of transition. Perhaps, time-dependent instabilities are the likely mechanism by which an attractor remains strange. The arguments leading towards the concept of strange attractors and the Ruelle-Takens theory of turbulence will become evident in the section on results and their discussion.

K. Ghia, Osswald and U. Ghia (1985a) analyzed massively separated flow past a 12 percent thick Joukowski airfoil using a symmetric C-grid. The Reynolds number ranged from 10^3 to 10^4 and the angle of attack α was varied up to 10°. For the configuration of Re = 10^3, α_f=15°, the unsteady massively separated flow asymptoted to a limit cycle. Subsequently, Osswald, K. Ghia and U. Ghia (1985b) significantly improved the above analysis by introducing circulation in the computation of conformal clustered C-grid. This resulted in the branch cut approaching the wake centerline a few chords downstream of the trailing edge (TE). A numerical method was developed to treat the branch cut of the C-grid implicitly while also appropriately treating the vorticity singularity at the TE. The versatility and efficiency of the numerical method were demonstrated by providing the massively separated flow structure for Re=10^3 and α_f=30° and also the transient results, at early times, for Re=10^3 and α_f=53°. The present study is a sequel to these earlier studies and has the following objectives:

i. To provide the detailed flow structure of massively separated flow for Re=10^3, α=53°, in the post-stall regime of the flow past a Joukowski airfoil,

ii. to obtain time-dependent aerodynamic lift, drag and moment coefficients for Re=10^3 and α_f between 15° to 53° and, finally,

iii. to understand the observed quasiperiodicity and bring forth any similarity possible with strange attractors.

ON THE ANALYSIS AND NUMERICAL METHODS

The conservative form of the unsteady Navier-Stokes equations in terms of vorticity and stream function in generalized curvilinear coordinates (ξ^1, ξ^2) is used. The far-field boundary conditions of uniform flow are, strictly, valid only at infinity. To circumvent the large values of ψ occurring in the far-field and also facilitate the numerical implementation of the far-field boundary conditions, the stream function ψ is decomposed into two parts such that $\psi = \psi_{in} + \psi_v$, neither of which need to be small in comparison to the other. Here, ψ_{in} is a solution of the stream function equation with zero vorticity and satisfies the free-stream condition at infinity and zero normal velocity at the surface of the airfoil. This decomposition is used so as to enable the far-field boundary condition to be placed at infinity for the viscous-flow calculations.

The Reynolds number used in this study is defined as $Re = U_\infty c/\nu$ where c is the airfoil chord. The characteristic time is given as $t = t^*/(c/U_\infty)$, with U_∞ being the undisturbed free-stream velocity. The boundary conditions correspond to uniform flow at infinity, together with the no-slip conditions along the body surface. The initial conditions for the viscous flow are taken as the corresponding steady-state inviscid solution.

A clustered conformal grid is generated; the clustering is controlled by appropriate one-dimensional (1-D) stretching transformations. An attempt is made to resolve many of the multiple scales of the unsteady flow with massive separation, while maintaining the transformation metrics to be smooth and continuous in the entire flow field. Typical clustered conformal grids consisting of (230, 46) points for a 12 percent thick symmetric Joukowski airfoil with α_g = 15°, 30° and 53° are shown in Fig. 1. Here, α_g is the grid angle of attack, i.e. the asymptotic slope of the coordinate line emanating from the TE; this may, or may not, be the same as the flow angle of attack α_f.

A fully implicit time-marching method is developed such that all spatial derivatives are approximated using central differences and no use is made of any artificial dissipation. The numerical method solves the discretized equations using the alternating-direction implicit-block Gaussian elimination (ADI-BGE) method and has overall $O[\Delta t, (\Delta\xi^1)^2, (\Delta\xi^2)^2]$ accuracy. The boundary conditions on the vorticity are so implemented as to maintain second-order spatial accuracy. The results obtained for this study are discussed next.

RESULTS AND DISCUSSION

A 12 percent thick symmetric Joukowski airfoil is used in this study and has two especially attractive features. (i) The Joukowski airfoil can be accurately represented using conformal transformations; the details of these and the clustering transformations used were given by Osswald, K. Ghia and U. Ghia (1985a). (ii) The presence of a sharp TE leads to a much stronger interacting region and, hence, truly

tests the analysis developed. This unsteady Navier-Stokes analysis and the corresponding numerical method are used to study three flow configurations in detail. All of these configurations have the same Re = 1,000 but the value of the free-stream incidence varies such that α_f = 15°, 30° and 53°, respectively. As stated earlier, a C-grid with (230x46) mesh points has been used; this number was arrived at based on the available full-core capacity of the supermini Perkin Elmer 3250 MPS computer system; this then also precluded a mesh refinement study. Hence, an attempt* was made to convert the program to run on the CYBER 205 VPS/32 computer at NASA Langley Research Center; this effort is still in progress. The CPU time τ require to advance the solution by one time step per spatial grid point is referred to as a "computational effort" index; the value achieved for τ was 2.14×10^{-3} seconds for a Perkin Elmer 3250 MPS supermini computer system.

Flow in Post-Stall Regime: Re = 1000, α_f = 53°

There are two critical parameters in the flow past an airfoil, namely, Re and α_f. In the present study, Re is held constant and only α_f is increased from 15° to 53°, so that α_f becomes the critical parameter in this discussion. For the high angle-of-attack case with α_f= 53°, the Joukowski airfoil appears, to the oncoming stream, as an apparent bluff body. The massively separated vortex-dominated flow in the post-stall regime for this configuration of the Joukowski airfoil, is exceedingly complex and, from the results available so far, it is feasible to conjecture two hypotheses; see Fig. 5. One possibility is that the solution has still not asymptoted to an exact limit cycle but may do so subsequently. The second possibility, based on the results for α_f = 30 to be discussed later, is that the solution may asymptote to a quasiperiodic state, with anywhere from 3 to 8 incommensurate frequencies. The second hypothesis is more likely to prevail and some arguments in its favor will be presented later. However, the discussion for this configuration is presently considered speculative in nature, since the results in Fig. 5 do not permit identifying a limit-cycle and describing its evolution. Hence, the time instants at which the results are presented, are selected arbitrarily to show the spatial structure between the LE-TE-LE sheddings.

The instantaneous stream function contours presented in Figs. 2a, c, e, g show massively separated flow with large eddies present over the suction surface as well as in the wake. The stagnation streamline on the pressure surface fluctuates and is closer to LE when the LE eddy is stronger in strength (see Fig. 2a) as compared to Figs. 2c, e where the clockwise rotating eddy has already been shed and is in the process of strong interaction with the counterclockwise eddy from the TE. The corresponding vorticity contours are shown in Figs 2b, d, f, h and are of greater

---

* This effort was made in August 1985, while the present investigators were in residence at ICASE. Subsequently, the computer program has been made fully operational and, it is anticipated that the much-needed grid refinement in the normal direction will be carried out shortly.

significance, since they are independent of the observer's reference frame and, hence, permit more meaningful assessment of the convection and diffusion of the vortices. Figure 2b shows the intense TE vortex and also the weaker LE vortex. As compared to the cases with α_f = 15° and 30°, the interaction between these two vortices is initially of a weaker nature.

Figure 2d corresponds to intense interaction between the LE vortex and a part of the TE vortex, while the remaining part of the TE vortex is elongated and its shedding is imminent. Still there is a substantial strength elongated vortex that has remained as seen in Fig. 2f and it is about to shed at t = 52.7; also, the shear layer from the LE has thickened. Finally, in Fig. 2h, both the LE and TE vortices are beginning to intensify and the earlier interacting vortices are on the verge of separating from the LE shear layer. The subsequent flow structure at t = 54.5, not shown here, is very similar to that at t = 50.4 and corresponds to shedding of the vortex at the LE. This evolution process could have been visualized more clearly, had color contour plots been available to distinguish the LE and TE vortices.

Limit Cycle Analysis

i. Coefficients of Lift, Drag and Moment for Re = 1000, α_f= 15°, 30° and 53°

Originally, the aerodynamic coefficients were computed only at intervals of 0.1 characteristic time. This was quite satisfactory for qualitative assessment of the flow evolution but too coarse for its detailed analysis. Subsequently, the computer program has been modified to provide the coefficients of lift C_L, drag C_D and moment C_M (nose-up positive about the quarter chord point) at every Δt increment. The configuration with α_f = 15°, which requires minimum time to reach the time-asymptotic limit cycle solution has been completely recomputed, using a slightly improved grid near the TE. The flow configuration with α_f = 30° has been recomputed between t = 45 and t = 58, whereas, due to limitation of availability of CPU time on host computer system, the configuration with α_f = 53° is currently available with C_L, C_D and C_M computations at the interval of 0.1t only. Figures 3a, b, c show C_L, C_D and C_M corresponding to α_f=15°. As seen in this figure, C_L rises initially but drops very sharply during the transient phase and asymptotes to a near-limit-cycle solution corresponding to the dominant frequency for the shedding of vortices from the TE. The L_2 norm of the entire vorticity and stream function fields were carefully examined to ensure that the near-limit-cycle has been achieved. This limit-cycle solution is an "ordinary attractor", the attractor being the 1-D object to which the phase-space trajectories are attracted at all times. The complete motion is known once the geometry of the attractor is determined. Hence, it is also possible to compute the mean flow by averaging the flow over one complete cycle; similarly, it is possible to determine the Reynolds stresses from first principles, although these computations have not been performed in the present study.

For the flow configuration with α_f=30°, the physics changes dramatically, as seen in Figs. 4a, b, c. The curves for the force coefficients show that one limit

cycle consists of two TE vortices sheddings. There are now two shedding frequencies, or modes, associated with this more complex attractor. As shown in Fig. 4a, the first frequency is associated with the shedding which takes place at point 1, whereas the second frequency is associated with the shedding which takes place at point 3. The LE shear layer associated with the first frequency is thinner and more intense, as compared to that associated with the second frequency. The energy now oscillates between the two unstable modes through a nonlinear coupling. The appearance of subharmonics signifies small modulations in the shedding frequency. This flow field, with its two natural incommensurate frequencies, is referred to as a quasiperiodic flow, also known as "Hopf bifurcation" into an invariant torus. From Fig. 4a, it is clear that the initial state at point 10 of a new cycle is slightly different from that at point 8. If the phase-space trajectories were drawn, this solution may very well show the tendency to fill a rather significant surface area of the torus. Finally, it should be noted that the C_D peaks in Fig. 4d correspond to points 2 and 9 in Fig. 4a.

For the case with α_f=53°, the results obtained up to t=74 may be far from approaching an asymptotic state. Figure 5a shows some resemblance of quasiperiodic flow with three incommensurate frequencies, this fact being further supported by the curves in Figs. 5b, c. From their numerical experiments, Grebogi, Ott and Yorke (1983) have also shown the existence of quasiperiodicity with three incommensurate frequencies. The state of the system at a given time instant in one cycle is not quite repeated at the corresponding time instant in the subsequent cycle. The phase-space portrait, not shown here, is very complex, where the surface has folded repeatedly onto itself, so that it appears to be a strange attractor. This is an indication, although preliminary, that the flow may be exhibiting a route to chaos. There are a few rigorous approaches to characterize a strange attractor. These are the determination of (i) the Lyapunov exponent, (ii) the fractal dimension of the attractor, which is related to the number of degrees of freedom; and finally, (iii) the Kolmogorov entropy. These indices still need to be studied thoroughly in order to rigorously analyze the route to chaos in a meaningful way.

ii. Entire State of the System

Analysis of lift, drag and moment histories by themselves is not sufficient to examine limit-cycle behavior since it is quite possible that two different dynamic states of the system may produce the same values of C_L, C_D and C_M. To avoid such a possibility, the L_2 norms of the difference between the evolving stream function and vorticity fields and their corresponding values at some designated initial time were computed at each time step. Only when this measure of the internal dynamic state of the system reached a value below a specified tolerance, was it considered that an initial state of the system had actually re-occurred. To date, this analysis has been carried out only for the configuration with Re=1,000 and α_f=15°. Here, a near-limit-cycle (within the specified tolerance) does occur, with a period of 1.416

characteristic-time units and a nondimensional shedding frequency of 0.706. The corresponding Strouhal number, $S = fc \sin\alpha/U_\infty = 0.18$, (see K. Ghia, Osswald and U. Ghia (1985b)), agrees well with the universal wake-based number of Roshko (1954). From Figs. 6a and c, as well as 6b and d, it is clear that the large as well as small-scale motion repeats itself and that a limit cycle has been nearly established. For the case of Re=1000 and α_f=30°, the L_2-norm of the solution has yet to be examined. Instead, the limit cycle was arrived at from visual observation of the variation of aerodynamic coefficients presented in Fig. 4. As seen in Fig. 4a, the two Strouhal numbers are S=0.15 and S=0.20, corresponding to two shedding frequencies. Considering the two sheddings per cycle, the overall Strouhal number S is obtained as 0.17 which, again, is in the correct range. The stream-function and vorticity contours in Figs. 7a-d for t=45.1 closely resemble those at 50.98, but the two states are not identical, implying a slightly different initial state each time. Finally, for Re=1000 and α_f=53°, the results obtained so far are not sufficient to warrant a limit-cycle analysis. It is likely that the flow field may asymptote to quasiperiodicity with three incommensurate frequencies, as can be inferred from Fig. 5b. However, this is a very weak justification and, hence, no attempt is made to compute the Strouhal number yet. In order to understand the degree to which this motion repeats itself, points 1 and 14, corresponding to LE shedding after three sheddings, have been plotted in Figs. 8a-d at t=46.2 and 58.6. The stream-function and vorticity contours are similar, but there are sufficient differences. This leads to the conjecture that the motion may be quasiperiodic with three frequencies, and may be on the route to chaos.

CONCLUSION

The unsteady Navier-Stokes analysis is shown to be capable of analyzing the massively separated, persistently unsteady flow in the post-stall regime of a Joukowski airfoil for angle of attack as high as 53°. The analysis has provided the detailed flow structure, showing the complex vortex interaction for this configuration. The aerodynamic coefficients, C_L, C_D and C_M for lift, drag and moment, respectively, have been calculated; these aid further in characterizing this unsteady flow. The use of α_f as the critical parameter appears to be appropriate, but further computations are needed to convincingly demonstrate the state of the flow for α_f=53°. The phase-space portrait not shown for this case does, at least qualitatively show that the asymptotic solution is a strange attractor. This study has so far only computed the spatial structure of the vortex interaction. It is now important to potentially use the large-scale vortex interactions, an additional energy source, to improve the aerodynamic performance. To achieve this, a quantitative analysis must be carried out from the results obtained so far to analyze the dependence of vortex evolutions, their growth and strength, and the various interactions amongst vortices and with the airfoil. This latter study would

aid in carefully characterizing the flow field as a function of the airfoil geometry. It is only after this phase that the undesirable aerodynamic features can be appropriately controlled and the energy of the unsteady vortex-dominated flow harnessed to improve the aerodynamic performance as desired under critical operating conditions.

REFERENCES

Ghia, K.N., Osswald, G.A. and Ghia, U. (1985a), "Analysis of Two-Dimensional Incompressible Flow Past Airfoils Using Unsteady Navier-Stokes Equations," Proceedings of Third Symposium on Numerical and Physical Aspects of Aerodynamic Flows, Long Beach, California.

Ghia, K.N., Osswald, G.A. and Ghia, U. (1985b), "Analysis of Two-Dimensional Incompressible Flow Past Airfoils Using Unsteady Navier-Stokes Equations," to appear in Numerical and Physical Aspects of Aerodynamic Flows, Editor: T. Cebeci, Springer Verlag, New York.

Grebogi, C., Ott, E. and Yorke, J.A. (1983), "Are Three-Frequency Quasiperiodic Orbits to be Expected in Typical Nonlinear Dynamical Systems?" Physcial Review Letters, Vol. 51, No. 5, pp. 339-342.

Osswald, G.A., Ghia, K.N. and Ghia, U. (1985a), "A Clustered Conformal Grid Generation Technique for Symmetric Joukowski Airfoils at Arbitrary Angle of Attack," AFL Report 85-1-69, University of Cincinnati, Cincinnati, Ohio.

Osswald, G.A., Ghia, K.N. and Ghia, U. (1985b), "An Implicit Time-Marching Method for Studying Unsteady Flow with Massive Separation," AIAA CP 854, pp. 25-37.

Roshko, A. (1954), "On Drag and Shedding Frequency of Two-Dimensional Bluff Bodies," NACA TN-3169.

Ruelle, D. and Takens, F. (1971), "On the Nature of Turbulence," Commun. Math. Phys., Vol. 20, pp. 167-192.

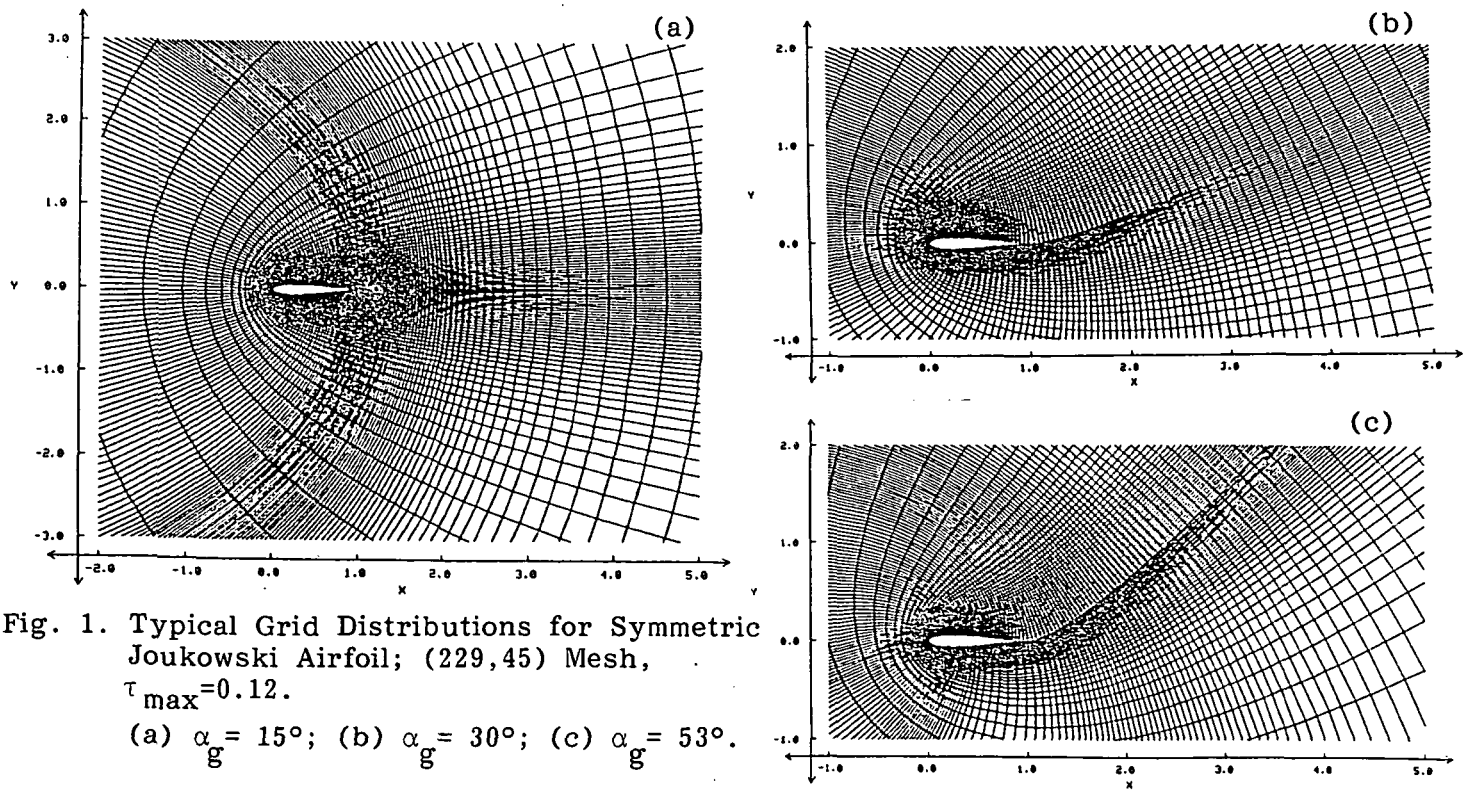

Fig. 1. Typical Grid Distributions for Symmetric Joukowski Airfoil; (229,45) Mesh, $\tau_{max}=0.12$.
(a) $\alpha_g = 15°$; (b) $\alpha_g = 30°$; (c) $\alpha_g = 53°$.

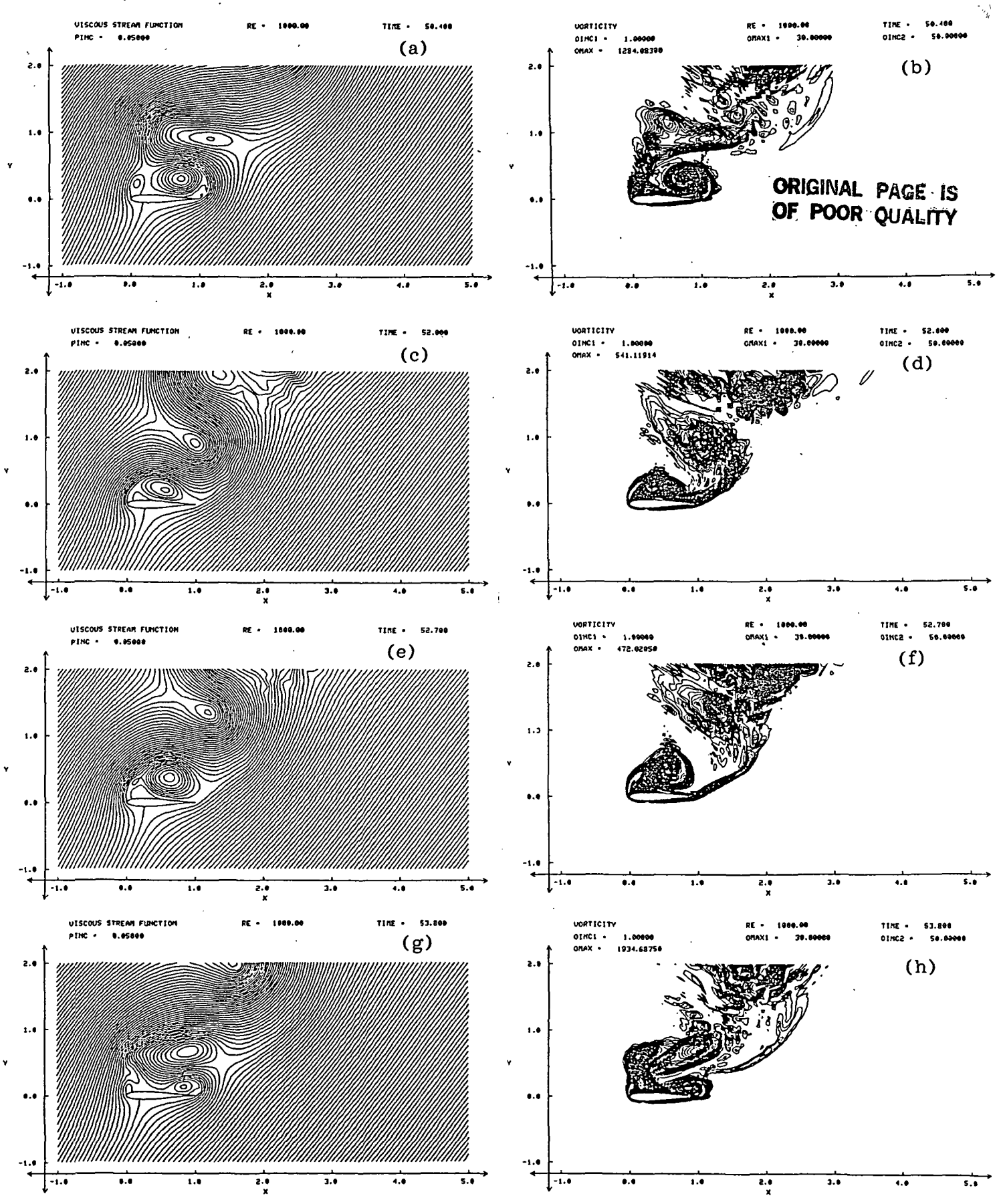

STREAM-FUNCTION CONTOURS VORTICITY CONTOURS

Fig. 2. LE-TE-LE Vortex-Shedding Cycle for Joukowski Airfoil at Re = 1,000, $\alpha_f = 53°$.

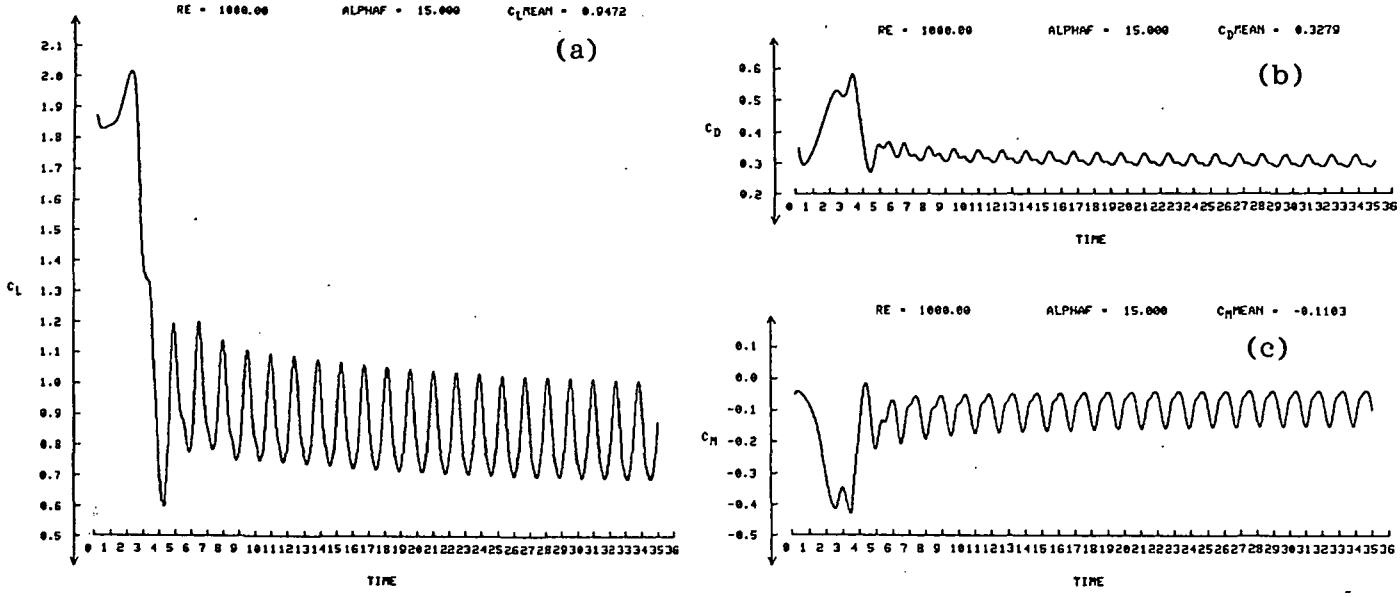

Fig. 3. Instantaneous Aerodynamic Coefficients at Re = 1,000, $\alpha_f = 15°$.
(a) Lift C_L, (b) Drag C_D, (c) Moment C_M.

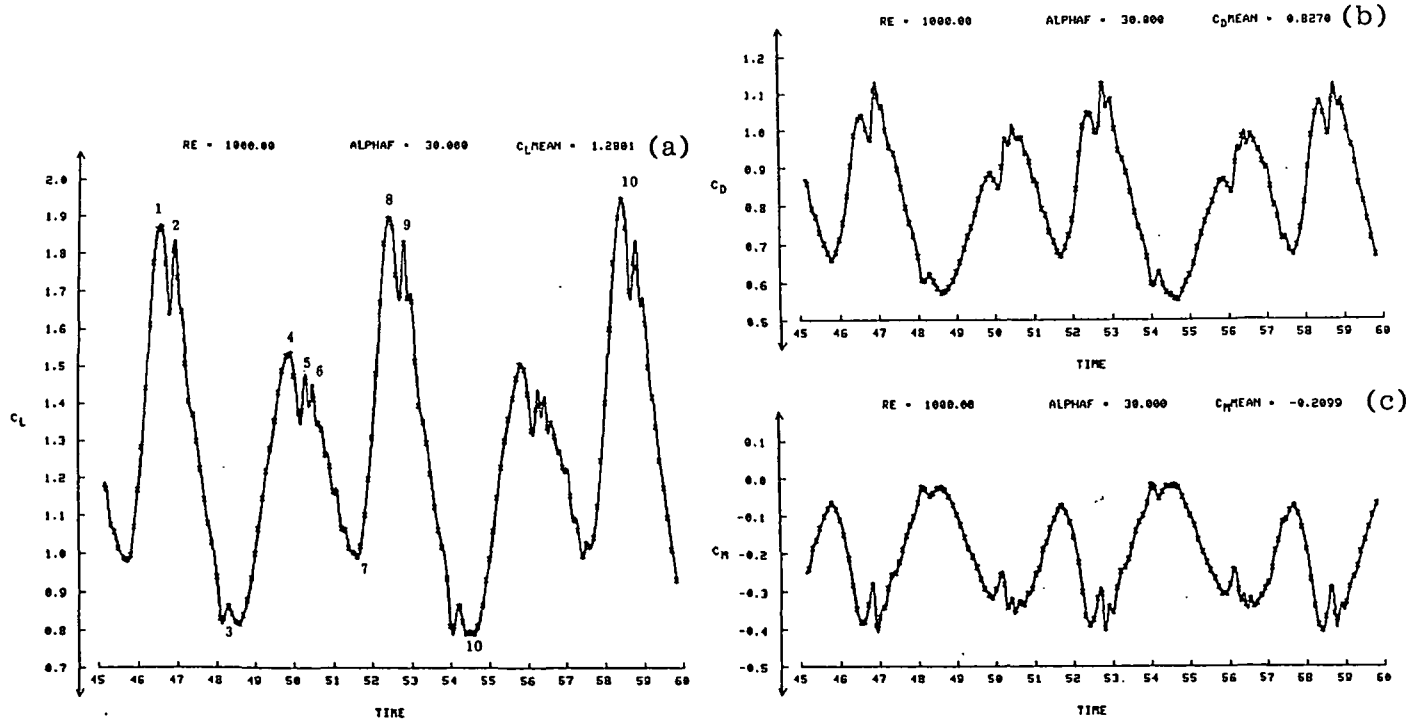

Fig. 4. Instantaneous Aerodynamic Coefficients at Re = 1,000, $\alpha_f = 30°$.
(a) Lift C_L, (b) Drag C_D, (c) Moment C_M.

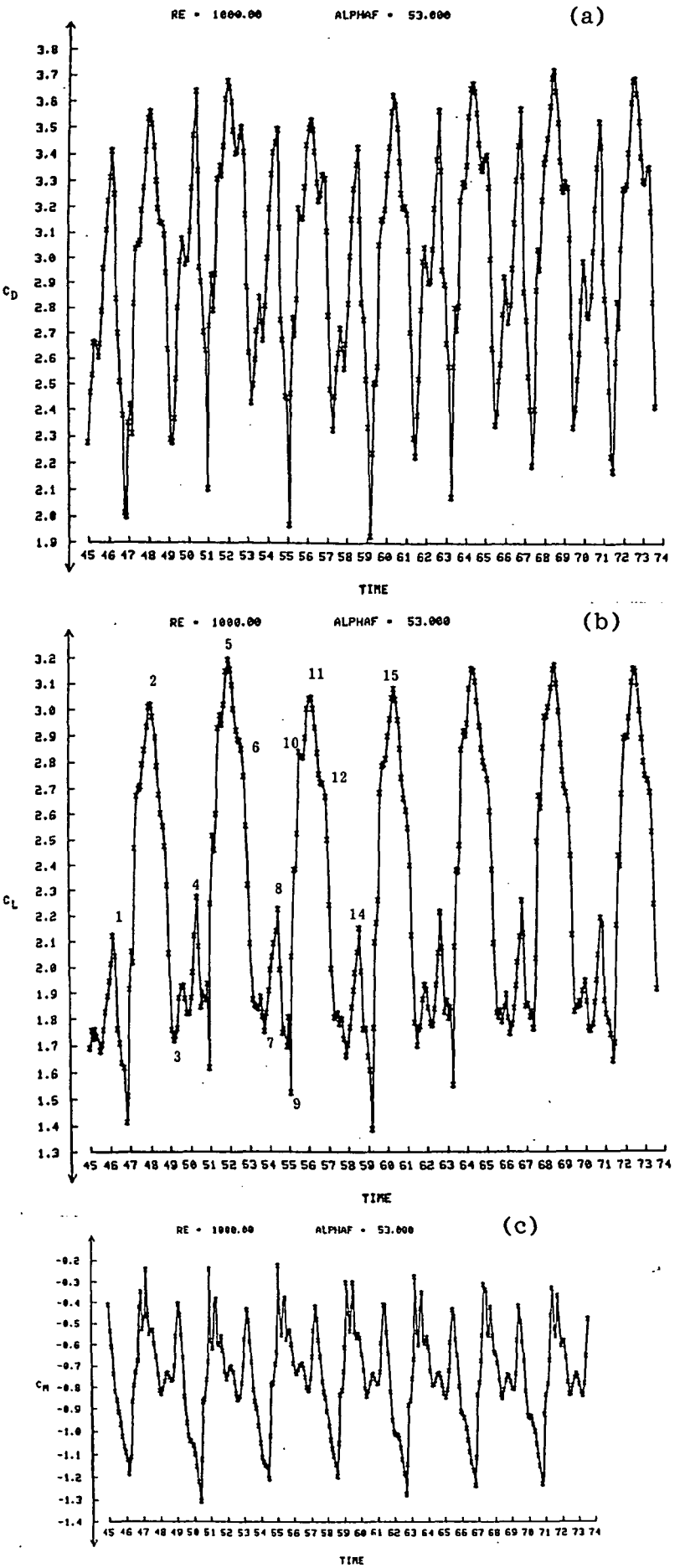

Fig. 5. Instantaneous Aerodynamic Coefficients at Re = 1,000, $\alpha_f = 53°$.
(a) Lift C_L, (b) Drag C_D, (c) Moment C_M.

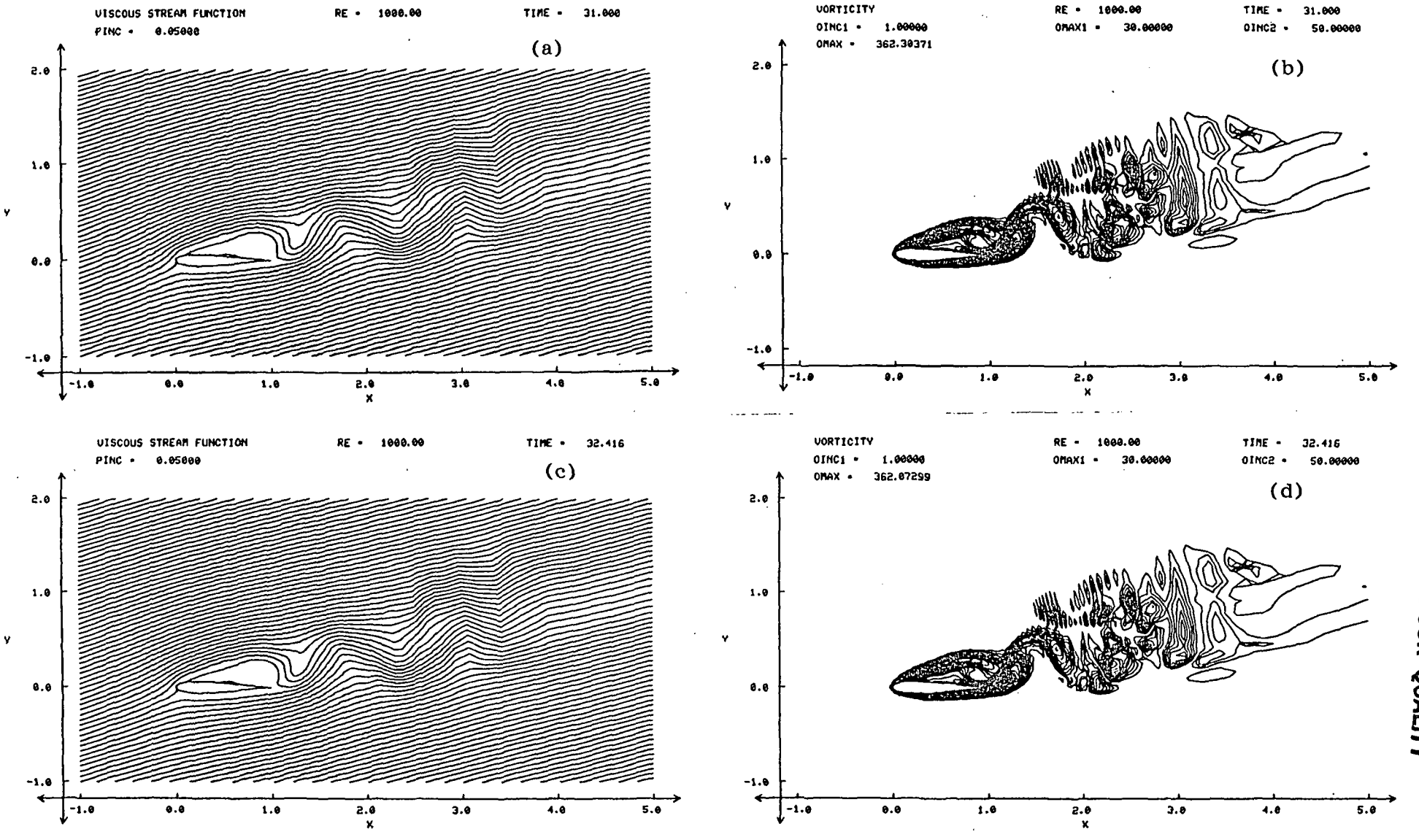

STREAM-FUNCTION CONTOURS

VORTICITY CONTOURS

Fig. 6. Limit-Cycle Analysis for Joukowski Airfoil at Re = 1,000, $\alpha_f = 15°$, S = 0.18.

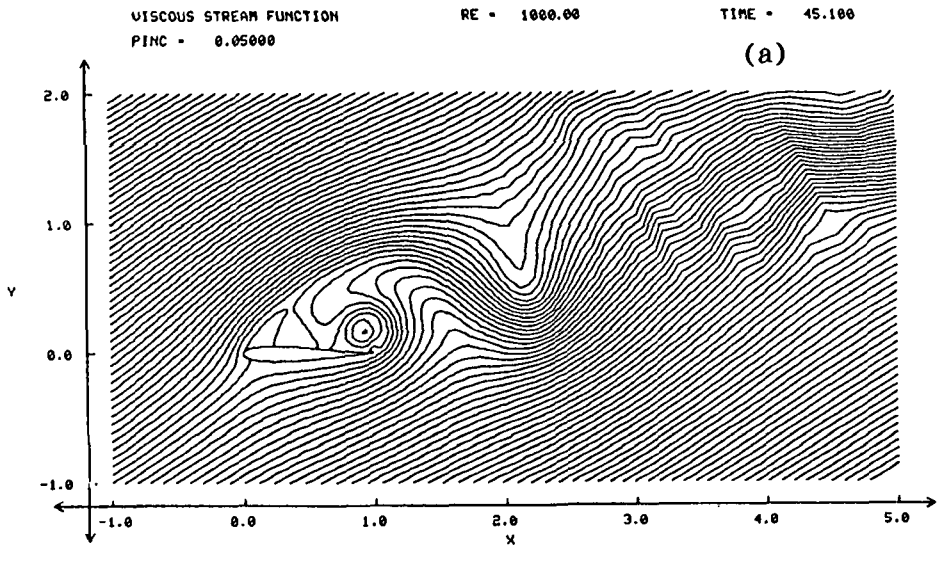

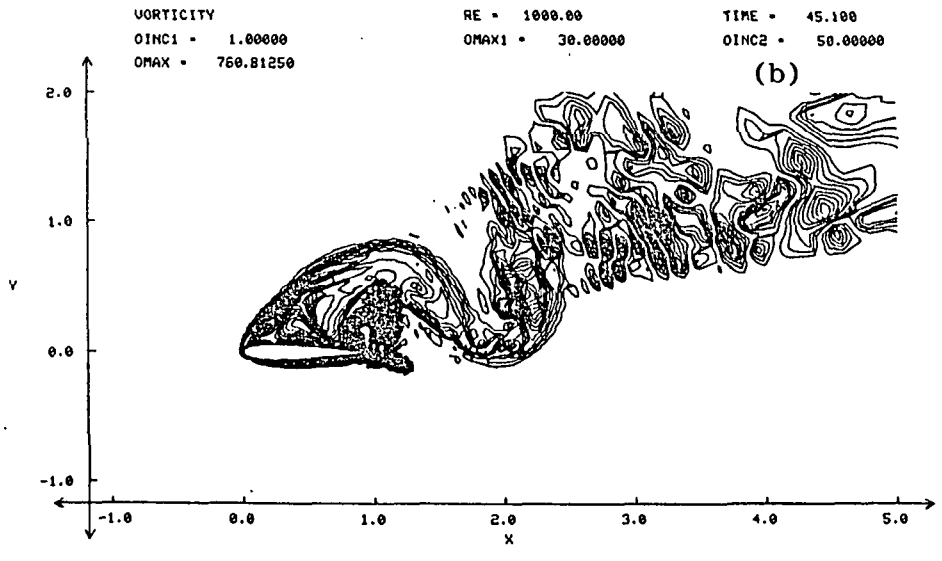

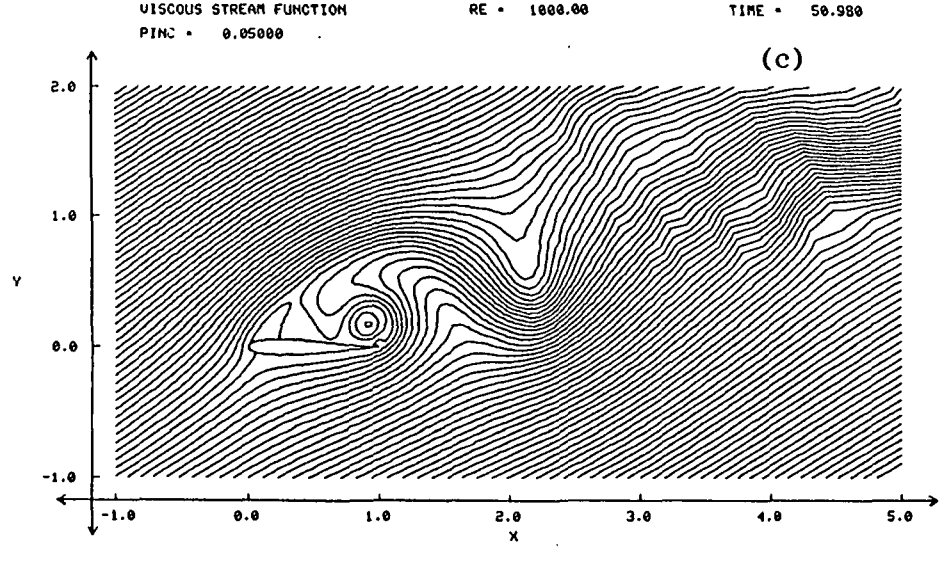

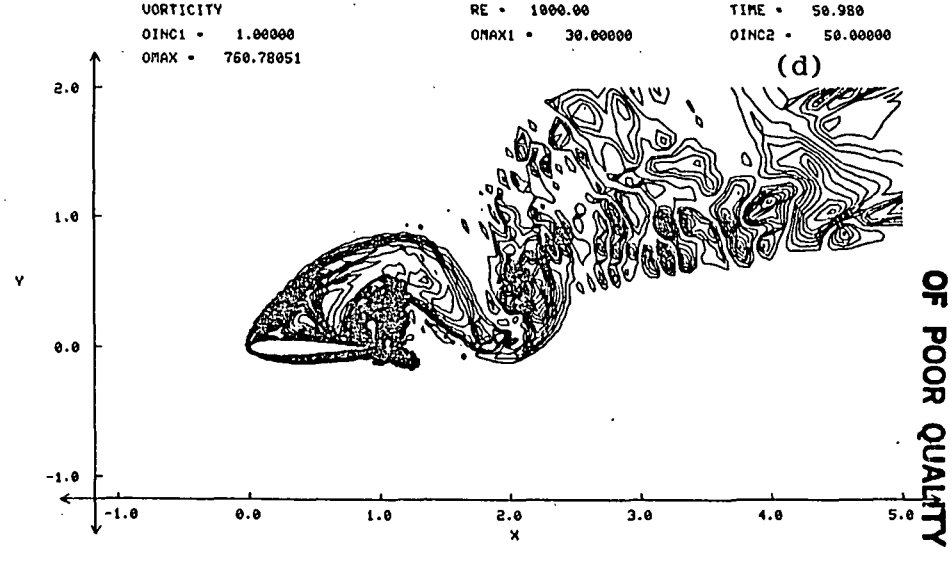

STREAM-FUNCTION CONTOURS

VORTICITY CONTOURS

Fig. 7. Limit-Cycle Analysis for Joukowski Airfoil at Re = 1,000, $\alpha_f = 30°$, S = 0.17.

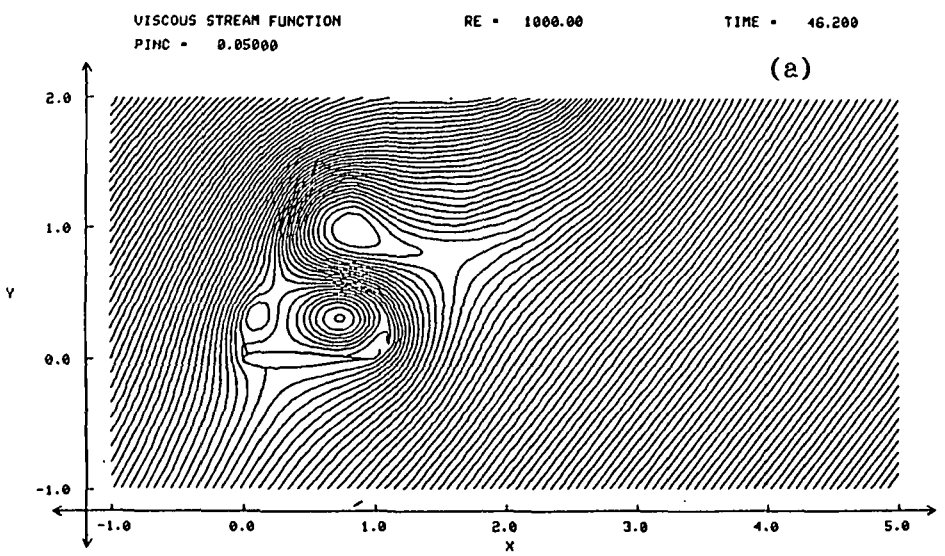

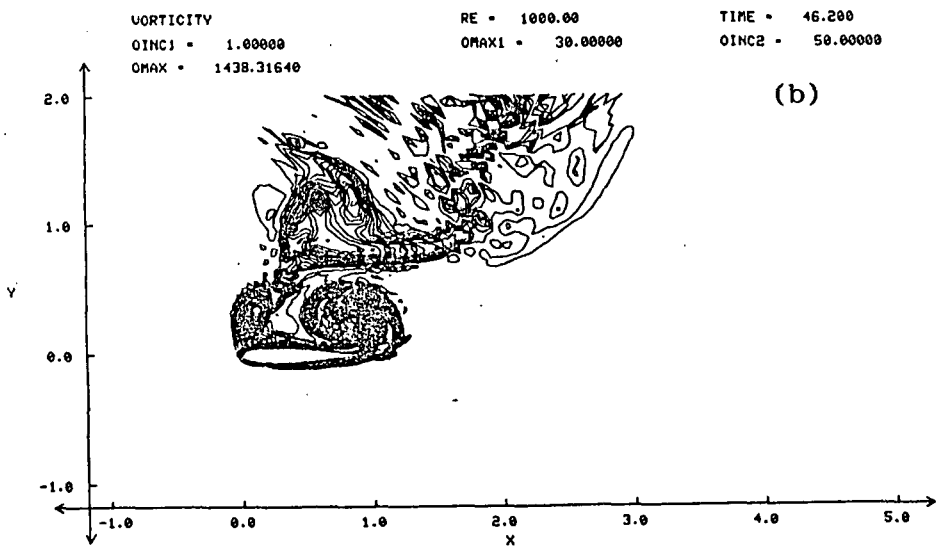

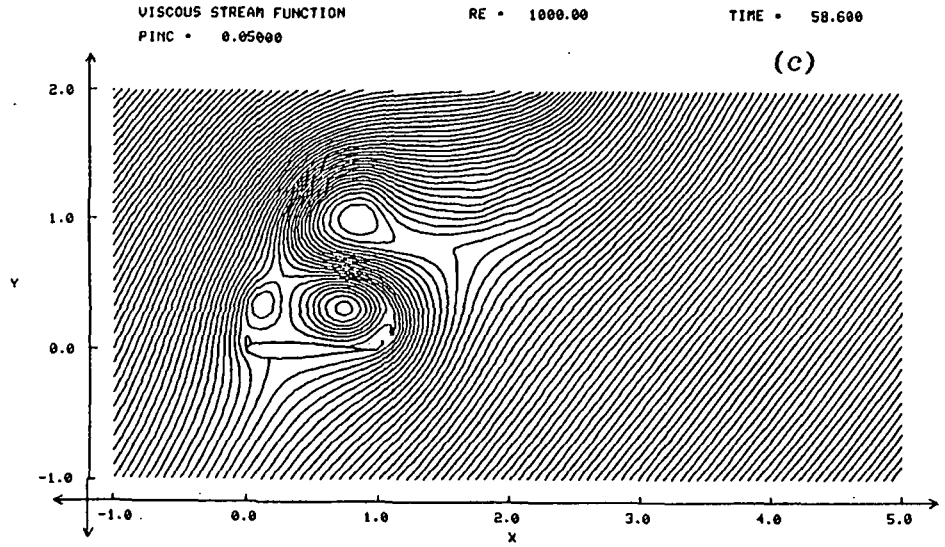

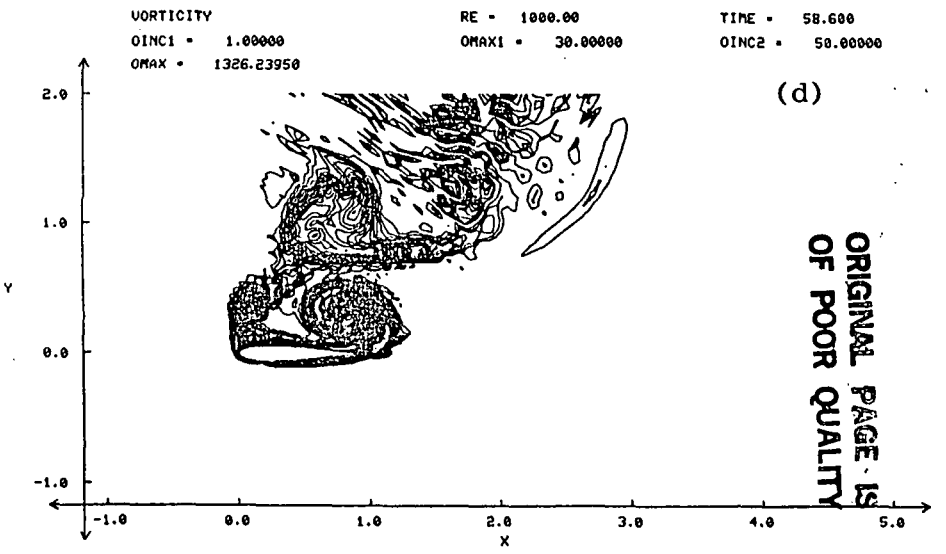

STREAM-FUNCTION CONTOURS

VORTICITY CONTOURS

Fig. 8. LE-TE-LE Vortex Shedding for Joukowski Airfoil at Re = 1,000, $\alpha_f = 53°$.